JACS
JOURNAL OF THE AMERICAN CHEMICAL SOCIETY

Article

pubs.acs.org/JACS

Quantifying Functional Group Interactions That Determine Urea Effects on Nucleic Acid Helix Formation

Emily J. Guinn,[†,∥] Jeffrey J. Schwinefus,[§,∥] Hyo Keun Cha,[‡,∥] Joseph L. McDevitt,[§] Wolf E. Merker,[§] Ryan Ritzer,[§] Gregory W. Muth,[§] Samuel W. Engelsgjerd,[§] Kathryn E. Mangold,[§] Perry J. Thompson,[§] Michael J. Kerins,[‡] and M. Thomas Record, Jr.*[,†,‡]

Departments of [†]Chemistry and [‡]Biochemistry, University of Wisconsin—Madison, Madison, Wisconsin 53706, United States
[§]Department of Chemistry, St. Olaf College, Northfield, Minnesota 55057, United States

Supporting Information

ABSTRACT: Urea destabilizes helical and folded conformations of nucleic acids and proteins, as well as protein−nucleic acid complexes. To understand these effects, extend previous characterizations of interactions of urea with protein functional groups, and thereby develop urea as a probe of conformational changes in protein and nucleic acid processes, we obtain chemical potential derivatives ($\mu_{23} = d\mu_2/dm_3$) quantifying interactions of urea (component 3) with nucleic acid bases, base analogues, nucleosides, and nucleotide monophosphates (component 2) using osmometry and hexanol−water distribution assays. Dissection of these μ_{23} values yields interaction potentials quantifying interactions of urea with unit surface areas of nucleic acid functional groups (heterocyclic aromatic ring, ring methyl, carbonyl and phosphate O, amino N, sugar (C and O); urea interacts favorably with all these groups, relative to interactions with water. Interactions of urea with heterocyclic aromatic rings and attached methyl groups (as on thymine) are particularly favorable, as previously observed for urea−homocyclic aromatic ring interactions. Urea *m*-values determined for double helix formation by DNA dodecamers near 25 °C are in the range of 0.72−0.85 kcal mol^{-1} m^{-1} and exhibit little systematic dependence on nucleobase composition (17−42% GC). Interpretation of these results using the urea interaction potentials indicates that extensive (60−90%) stacking of nucleobases in the separated strands in the transition region is required to explain the *m*-value. Results for RNA and DNA dodecamers obtained at higher temperatures, and literature data, are consistent with this conclusion. This demonstrates the utility of urea as a quantitative probe of changes in surface area (ΔASA) in nucleic acid processes.

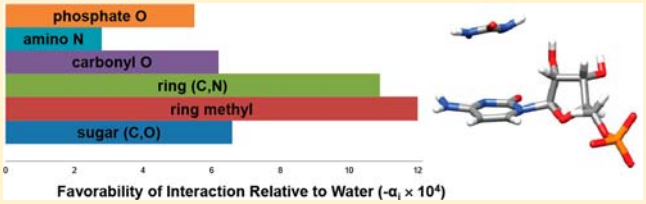

1. INTRODUCTION

Noncovalent self-assembly and function of proteins and nucleic acids involve large-scale changes in water-accessible surface area (|ΔASA| ≫ 0). Solutes affect these processes because of their favorable or unfavorable interactions with the functional groups on the biopolymer surface that comprises the ΔASA. Once the interactions of solutes with protein and nucleic acid functional groups are quantified, these solutes can be used as probes to determine the amount and composition of the biopolymer surface exposed or buried in individual steps of a process.[1] Myers et al. observed that urea protein unfolding *m*-values (derivatives of the standard free energy change ΔG°_{obsd} for unfolding with respect to urea concentration) are approximately proportional to the change in water-accessible surface area (ΔASA) in unfolding, calculated using an extended chain model of the unfolded state.[2] Analysis of the effects of urea, other solutes, and Hofmeister salts on unfolding and other processes using the solute partitioning model (SPM) predicts the proportionality of solute *m*-values to ΔASA and demonstrates that the molecular basis of these thermodynamic effects is the accumulation (favorable interaction) or exclusion (unfavorable interaction, relative to that with water) of the solute or salt ion in the vicinity of the chemical functional groups exposed upon unfolding.[1,3−6]

The effects (*m*-values) of urea, glycine betaine (GB), and different Hofmeister salts on protein stability have been quantitatively interpreted in terms of the chemical interactions of these solutes and salt ions with the chemical functional groups exposed in unfolding (primarily aliphatic and aromatic hydrocarbon (∼70%, with ∼9:1 aliphatic:aromatic ratio) and amide oxygen and nitrogen (∼20%, with ∼2:1 O:N ratio)).[1,3−9] We recently quantified the preferential interactions of urea with the seven most significant protein functional groups (amide O and N, aliphatic and aromatic C, hydroxyl O, carboxylate O, cationic N) relative to interactions with water and found that urea interacts most favorably with amide O and aromatic C.[4] For amide O, this result indicates that hydrogen bonds formed with urea as the donor and amide O as the acceptor are more favorable than the corresponding hydrogen bonds with water; spectroscopic studies provide independent evidence for urea−amide hydrogen bonds.[10,11] Urea *m*-values for protein

Received: January 28, 2013
Published: March 19, 2013

   dx.doi.org/10.1021/ja400965n | J. Am. Chem. Soc. 2013, 135, 5828−5838

unfolding and other protein processes are quantitatively predicted using these data.[1,4] For globular protein unfolding, favorable interactions of urea with amide O, aromatic C, and aliphatic C groups exposed in unfolding are predicted to make similar contributions to the urea *m*-value.[4]

In this work, we determine the chemical and thermodynamic basis of urea destabilization of DNA and RNA structures. Urea lowers the transition temperature of nucleic acid secondary and tertiary structures;[12−16] for RNA duplexes, this destabilization has been correlated with the surface area exposed in the unfolding transition.[17,18] Urea does not affect the cooperativity of melting or the structure of the folded form.[17,19,20] While a perturbing effect of urea on stacking in single-stranded DNA/RNA would be expected, evidence for this has not been obtained (see the Results and Discussion).[17]

Carbonyl O and amino N groups on nucleic acid bases (nucleobases) are similar in hydrogen-bonding potential to amide O and N of proteins, and the heterocyclic aromatic ring is analogous to the homocyclic aromatic ring of Phe or Tyr. Nucleic acid melting exposes ASA that is approximately 30% C and 70% O and N,[1] the composition opposite that exposed in unfolding globular proteins, so interactions of urea with a polar (O, N) surface are expected to be more important determinants of the effect of urea on nucleic acid stability. By quantifying the interaction of urea with DNA and RNA backbone and nucleobase chemical functional groups, we gain insight into the molecular and thermodynamic origins of the effect of urea on DNA and RNA processes. Future comparative studies with primary and secondary amides will allow us to dissect these interactions into contributions from amide O and N and provide insight into the thermodynamic contributions of interactions of amide groups on proteins with nucleobases and the sugar−phosphate backbone of nucleic acids.

At subdenaturing concentrations, urea exhibits very large effects on protein−nucleic acid processes, including binding of the lac repressor protein to operator DNA[21] and the late steps in the mechanism of formation of a transcription complex between RNA polymerase and promotor DNA.[22] Knowledge of how urea interacts with both protein and nucleic acid functional groups is allowing us to predict and interpret the effect of urea on these processes in terms of interface formation and coupled folding or other conformational changes. In the longer term, urea will be used as one of a set of solute probes (including glycine betaine, proline, trifluoroethanol, glycerol, and tetraethylene glycol, once characterization of their interactions with protein and nucleic acid functional groups is complete) to quantify the amount and chemical composition of the ΔASA in individual steps of mechanisms of action of protein molecular machines.

Here we determine the interaction of urea with nucleic acid functional groups by quantifying the interactions of urea with model compounds representing nucleic acid surface types (nucleic acid bases/base analogues, nucleosides, and nucleotide monophosphates) using vapor pressure osmometry (VPO) and measurements of the distribution of nucleobase between water and hexanol. We dissect interactions into interactions with individual functional groups using an ASA-based analysis, which are interpreted in terms of noncovalent interactions.[4] We determine the effect of urea on RNA and DNA duplex formation and interpret the *m*-values using individual functional group interactions to gain insight into the conformational changes involved in this process.

2. THERMODYNAMIC BACKGROUND AND ANALYSIS

The effects of solutes on biopolymer processes such as nucleic acid helix formation in aqueous solution are quantified using *m*-values, derivatives of the standard free energy change ($\Delta G^\circ_{obsd} = -RT \ln K_{obsd}$) for the process with respect to the solute concentration:

$$m\text{-value} = \frac{\partial \Delta G^\circ_{obsd}}{\partial m_3} = -RT\frac{\partial \ln K_{obsd}}{\partial m_3} = RT\frac{\partial \ln K_\gamma}{\partial m_3}$$
$$= RT\Delta\left(\frac{\partial \ln \gamma_2}{\partial m_3}\right) = \Delta\frac{d\mu_2}{dm_3} = \Delta\mu_{23} \quad (1)$$

where K_{obsd} is the equilibrium concentration quotient of products and reactants in the process, K_γ is the corresponding quotient of activity coefficients (γ) describing the interaction of products and reactants with solutes, and μ_{23} is the chemical potential derivative (the subscripts 1, 2, and 3 refer to water, biopolymer/model compound, and urea, respectively, throughout this paper). The value of μ_{23} is a measure of the preferential interaction of a solute with a biopolymer or model compound, where a negative value indicates a favorable preferential interaction and a positive value indicates an unfavorable preferential interaction relative to interactions with water.

Values of μ_{23}/RT for interactions of urea with model compounds containing protein surface types have been obtained by solubility, micelle formation, or VPO assays;[4] none of these assays are useful to quantify interactions of urea with nucleobases and base analogues. Here, a two-phase assay is developed to measure $K_D^{WH} = (m_2^{hex}/m_2^{aq})_{eq}$, the distribution of a nucleic acid base or base analogue between hexanol- and water-rich solutions. Paralleling the thermodynamic analysis in eq 1

$$\frac{d \ln K_D^{WH}}{dm_3^{aq}} = \frac{\Delta\mu_{23}}{RT} \approx \frac{\mu_{23}^{aq}}{RT} \quad (2)$$

where m_3^{aq} is the urea concentration in the aqueous phase. The approximation in eq 2 is discussed in the Supporting Information.

Values of μ_{23}/RT for protein model compounds were dissected in an ASA-based analysis (motivated by refs 3 and 6) to determine interactions of urea with individual protein functional groups and inorganic ions.[4] Here, we use this same analysis to determine interactions of urea with individual nucleic acid functional groups by dissecting experimentally determined μ_{23}/RT values for the interaction of urea with Na_2NMPs, nucleosides, nucleobases, and base analogues determined by VPO and distribution assays into additive contributions from the interaction of urea with each nucleic acid functional group, as well as with the two Na^+ ions for the 5′-NMPs:

$$\frac{\mu_{23}}{RT} = \sum_i \alpha_i(\text{ASA})_i + \nu_{Na^+}\beta_{Na^+} \quad (3)$$

where α_i represents the contribution to μ_{23}/RT from the interaction of urea with a unit surface area of surface type *i*. The term $\nu_{Na^+}\beta_{Na^+}$ represents the contribution of ν Na^+ ions per formula unit (2 for the 5′-NMP salts, 0 for nonelectrolytes), where β_{Na^+} is the contribution of the interaction of urea with a Na^+ ion to μ_{23}/RT, determined by analysis of VPO data for the interaction of urea with sodium carboxylates, amino acids, and NaCl.[4] The assumption of additivity of contributions to μ_{23} is supported by recent studies of interactions of Hofmeister salts,[5]

dx.doi.org/10.1021/ja400965n | J. Am. Chem. Soc. 2013, 135, 5828−5838

urea,[4] and glycine betaine[6] with model compounds displaying the functional groups of proteins, as well as interactions of oligomers of ethylene glycol with the surface exposed in melting nucleic acid oligomers.[23] Deviations from additivity are of interest as examples of context dependence arising from simultaneous interactions of a solute with two or more functional groups on the model compound or biopolymer.

3. EXPERIMENTAL SECTION

3.1. 5′-NMP Vapor Pressure Osmometry. Details of the sample preparation are described in the Supporting Information. A Wescor Vapro 5520 vapor pressure osmometer operating at ambient temperature was calibrated using standard osmolality solutions from Wescor. All osmolalities were corrected for discrepancies between accepted literature values and the Wescor standard solutions of sodium chloride.[24] Triplicate osmolality measurements were made on each sample and the standard errors determined as by Hong et al.[24]

Values of μ_{23} for urea (component 3)−Na_2NMP (component 2) interaction at constant NaCl (component 4) concentration were obtained from osmolality data on four-, three-, and two-component solutions as follows:

$$\Delta\mathrm{Osm} \cong \left(\frac{\mu_{23}}{RT}\right) m_2 m_3 \tag{4}$$

where

$$\Delta\mathrm{Osm}_{23,4} = (\mathrm{Osm}(m_2, m_3, m_4) - \mathrm{Osm}(m_2, m_4)) - (\mathrm{Osm}(m_3, m_4) - \mathrm{Osm}(m_4)) \tag{5}$$

This generalization of the three-component ΔOsm equation to the situation where a constant background of a fourth component (here NaCl) is present was previously used for DNA osmometry by Hong et al.[25] Error propagation in $\Delta\mathrm{Osm}_{23,4}$ used eq 3.13 of Bevington and Robinson[26] with standard errors and covariances of correlated parameters from multiple linear regression of the $\mathrm{Osm}(m_2,m_3,m_4)$ and $\mathrm{Osm}(m_3,m_4)$ data (eqs 7.14−7.17, 7.19, and 7.25 of Bevington and Robinson[26]). To check if urea has a significant effect on NaCl activity, μ_{34} was calculated as described in ref 23 using urea−salt data from ref 4 and found to be negligibly small (<4% of $\mu_{23,4}/RT$).

3.2. Nucleic Acid Base and Base Analogue Distribution Assay. A series of 10 mL aqueous urea solutions with concentrations ranging from 0 to 4 *m* were prepared gravimetrically. The nucleobase or base analogue was dissolved in hexanol, and 2 mL of this solution was added to each urea solution. The samples were incubated in a 25 °C shaking water bath for up to 24 h; the same concentration ratio was observed if the samples were read anywhere between 1 and 24 h after preparation. Absorbances of the water and hexanol phases were measured in a Cary 1 UV−vis spectrophotometer.

From these data, we determine the equilibrium constant (distribution coefficient) K_D^{WH} (eq 2) characterizing the distribution of the nucleobase between aqueous urea solutions and hexanol; absorbances (directly related to molar concentration) are converted to molal concentration to determine this molal scale concentration ratio as described in the Supporting Information. Values of μ_{23}/RT were determined from the initial slopes of plots of ln K_D^{WH} vs urea molality (eq 2). See Figure S1 (Supporting Information) for sample plots of $\ln(m/m^0)$ vs aqueous urea concentration for the hexanol and water phases and the resulting ln K_D^{WH} vs aqueous urea concentration plot. As controls for the validity of this assay and the approximation in eq 2, the results of the distribution assay are compared with the results of solubility assays for nucleobase−salt interactions and with VPO results for nucleoside−urea interactions in the Supporting Information.

3.3. DNA and RNA Dodecamer Thermal Denaturation and Urea Titration. Details of DNA and RNA dodecamer sample preparation are given in the Supporting Information. For thermal melts and urea titrations, dodecamer duplex transitions were monitored at 260 nm using a Cary 100 UV−vis spectrophotometer (Varian) equipped with a Peltier temperature controller. For thermal melts, dodecamer duplex samples were heated at a rate of 0.3 °C/min and absorbance readings were collected every 0.2 °C. For urea titrations, absorbance readings were collected as urea was added and the absorbance was normalized to molar DNA concentration. Dodecamer duplex and single-stranded baseline regions in the absorbance melting profiles were fit by linear regression (slopes were less than 1% of the overall absorbance change between duplex and single-stranded states); the fraction of single-stranded (f_{ss}) dodecamer was determined from the difference in absorbance between the experimentally measured values and the extrapolated baseline values.

The observed equilibrium constant K_{obsd} for duplex formation from the single strands S1 and S2 (S1 + S2 → duplex) can be determined from the total strand concentration ($[\mathrm{str}]_{tot} = [\mathrm{S1}] + [\mathrm{S2}] + [\mathrm{duplex}]$) and f_{ss}:

$$K_{obsd} = \left(\frac{[\mathrm{S1}][\mathrm{S2}]}{[\mathrm{duplex}]}\right)_{eq} = \frac{f_{ss}^{\,2}[\mathrm{str}]_{total}}{2(1-f_{ss})} \tag{6}$$

For titrations, K_{obsd} is determined over the range of urea concentrations where $0.2 < f_{ss} < 0.8$. For thermal melts, van't Hoff plots were made of $\ln(K_{obsd})$ vs $1/T$ in the T range where $0.2 < f_{ss} < 0.8$ (the slope is $\Delta H^\circ_{obsd}/R$). The value of K_{obsd} used in *m*-value analysis is interpolated from these plots at the temperature where $f_{ss} = 0.2$ in 0 *m* urea (this temperature is in the $0.2 < f_{ss} < 0.8$ transition region for all urea concentrations studied). Linear regression of the natural log of K_{obsd} with urea molarity was used to calculate the *m*-value (eq 1). Buffer and salt molalities were held constant in these experiments; urea has no effect on the salt dependence of DNA melting (Supporting Information).

3.4. ASA Calculations. 5′-NMP, nucleobase/base analogue, and nucleoside solvent-accessible surface areas (ASAs) were calculated using Surface Racer[27] with a probe radius of 1.4 Å and the set of van der Waals radii from Richards.[28] Coordinate files for the compounds were obtained from NMR solution structures from the Biological Magnetic Resonance Data Bank. The 5′-NMP nucleobases were in the *anti* conformation, although the difference in ASA between 5′-NMPs in either *syn* or *anti* conformation was less than 5%.

The DNA surface area newly exposed in unfolding (ΔASA) for each dodecamer duplex in Table 1 was calculated for three models of the single-stranded oligomers, assuming nucleobases were stacked, half-stacked, and fully unstacked.[25] The xleap module in AMBER 10[29] was used to construct the B- and A-forms of the DNA and RNA dodecamer duplexes, respectively. The ASAs of the duplex and two single strands in either the B-form (DNA) or A-form (RNA) conformation were calculated using naccess[30] with the same parameters used to calculate the 5′-NMP ASA. Single strands stripped out of helices in the B- or A-form have stacked nucleobases. To make unstacked strands, the torsion angles about the O3′−P bonds were rotated 120° in PyMol[31] to break up any nucleobase stacking starting at the 5′ end of the single strands. The ASA for a single strand in the half-stacked model was obtained by averaging the ASAs for stacked and unstacked single strands. The ΔASA for unfolding a duplex was then calculated by summing the ASAs of the two single strands and subtracting the ASA of the duplex.

3.5. Determining α_i Values. The ASAs of the 5′-NMPs, nucleobases/base analogues, and nucleosides are divided into six distinct surface types: anionic phosphate O, sugar C and O, heterocyclic aromatic ring C and N, and the functional groups on the heterocyclic rings (carbonyl O, amino N, aliphatic C). Even though the heterocyclic aromatic ring contains both C and N atoms, of necessity it is treated as one surface type because the ASA ratios of aromatic C/N are similar in all the model compounds we studied. Likewise, the ASA ratios of sugar C and O in all the nucleosides and nucleotides studied are similar, so they are treated as one surface type. We determine the ASA of each type of surface on the model compounds from structural data as described above.

Values of μ_{23}/RT for model compounds in Table 1 and model compound ASA data from Table S1 (Supporting Information) were globally fit to eq 3 using multiple linear regression in Igor 5.04B to

dx.doi.org/10.1021/ja400965n | J. Am. Chem. Soc. 2013, 135, 5828−5838

Table 1. Values of μ_{23}/RT for Interactions of Urea with Model Compounds

model compd	exptl μ_{23}/RT (m^{-1}) ± SD	predicted μ_{23}/RT (m^{-1}) ± SD
	Nucleobases	
cytosine	−0.17 ± 0.04	−0.19 ± 0.02
uracil	−0.22 ± 0.02	−0.22 ± 0.02
thymine	−0.23 ± 0.01	−0.26 ± 0.02
purine	−0.26 ± 0.01	−0.28 ± 0.02
adenine	−0.27 ± 0.01	−0.25 ± 0.02
hypoxanthine	−0.28 ± 0.01	−0.27 ± 0.02
theobromine	−0.37 ± 0.02	−0.35 ± 0.02
theophylline	−0.37 ± 0.02	−0.35 ± 0.02
caffeine	−0.40 ± 0.02	−0.40 ± 0.03
	Mononucleotides (Na_2NMP)	
$2Na^+ + 5'\text{-}CMP^{2-}$	−0.102 ± 0.014	−0.10 ± 0.04
$5'\text{-}CMP^{2-}$	−0.299 ± 0.031[a]	−0.30 ± 0.05
$2Na^+ + 5'\text{-}AMP^{2-}$	−0.126 ± 0.012	−0.16 ± 0.04
$5'\text{-}AMP^{2-}$	−0.323 ± 0.030[a]	−0.36 ± 0.05
$2Na^+ + 5'\text{-}GMP^{2-}$	−0.140 ± 0.016	−0.13 ± 0.04
$5'\text{-}GMP^{2-}$	−0.337 ± 0.032[a]	−0.33 ± 0.05
$2Na^+ + 5'\text{-}dTMP^{2-}$	−0.148 ± 0.013	−0.17 ± 0.04
$5'\text{-}dTMP^{2-}$	−0.345 ± 0.031[a]	−0.37 ± 0.05
$2Na^+ + 5'\text{-}UMP^{2-}$	−0.166 ± 0.012	−0.12 ± 0.04
$5'\text{-}UMP^{2-}$	−0.363 ± 0.057[a]	−0.32 ± 0.05
	Nucleosides	
guanosine	−0.31 ± 0.03	−0.31 ± 0.03
uridine	−0.31 ± 0.02[b]	−0.31 ± 0.03
deoxythymidine	−0.31 ± 0.02[c]	−0.33 ± 0.02
adenosine	−0.35 ± 0.02	−0.34 ± 0.03

[a]Determined by subtracting the contribution of interaction with $2Na^+$ ($2\beta_{Na^+} = 0.197 \pm 0.028\ m^{-1}$) predicted from model compound data in ref 4 from the experimental value. [b]Average of μ_{23}/RT values obtained from VPO ($-0.34 \pm 0.02\ m^{-1}$) and hexanol−water distribution assays ($-0.28 \pm 0.02\ m^{-1}$). [c]Average of μ_{23}/RT values obtained from VPO ($-0.33 \pm 0.03\ m^{-1}$) and hexanol−water distribution assays ($-0.29 \pm 0.02\ m^{-1}$).

determine α_i values for interaction of urea with individual nucleic acid functional groups. For the urea−Na^+ interaction, the value of β_{Na^+} ($0.099 \pm 0.014\ m^{-1}$) was determined from model compound data in ref 4 reanalyzed as described in the Supporting Information. Nucleobase and base analogue partitioning data were also fit to eq 3 as above without the nucleoside partitioning data or 5′-NMP VPO data. The resulting interaction potentials for the interactions of urea with surface types found on these nucleobases and analogues (ring methyl, aromatic ring, carbonyl O, amino N) were the same within error as those determined from the fit including the nucleoside and 5′-NMP data.

4. RESULTS AND DISCUSSION

4.1. Interactions of Urea with Model Compounds.

4.1.1. Distribution Studies. Interactions of urea with the sparingly soluble nucleosides and nucleic acid bases and base analogues were determined from the effect of the urea concentration on the distribution of the nucleobase between a hexanol-rich phase and predominantly aqueous urea solutions. In the absence of urea, all nucleobases and base analogues concentrate in the hexanol-rich phase; the distribution of the nucleobase is quantified by the water−hexanol distribution coefficient K_D^{WH}. Figure 1 plots the natural logarithm of K_D^{WH} (normalized to K_D^{WH} in the absence of urea) against the urea concentration (eq 2). The negative slopes here indicate that urea (which is concentrated in the aqueous phase; see the Supporting Information) increases the concentration of the nucleobase, base analogue, or nucleoside in the aqueous phase and therefore has a favorable interaction with these compounds, as is the case for interactions of urea with other nonelectrolytes studied.[4] Values of μ_{23}/RT were determined from initial slopes of quadratic fits to these plots (see the Supporting Information for details) and are summarized in Table 1. The distribution assay was adopted because most nucleosides and nucleobases/base analogues are too insoluble for VPO and too slow (∼2 weeks) to achieve solubility equilibrium before artifacts (perhaps arising from degradation of urea[32]) become significant. Long and McDevit[33] described the use of distribution assays to determine the effect of Hofmeister salts on nonpolar solute activity, which have been used to quantify the interaction of Hofmeister salts with formamide[34] and with nitrobenzoic acids, where the same results were obtained from solubility and distribution experiments.[35] Distribution assays of this type have also been used to quantify the hydrophobicity of carboxylic acids and nucleic acid bases from their distribution between heptane and water[36,37] and to estimate the solubility of various compounds in water from the correlation of solubility with octanol−water distribution coefficients.[38,39]

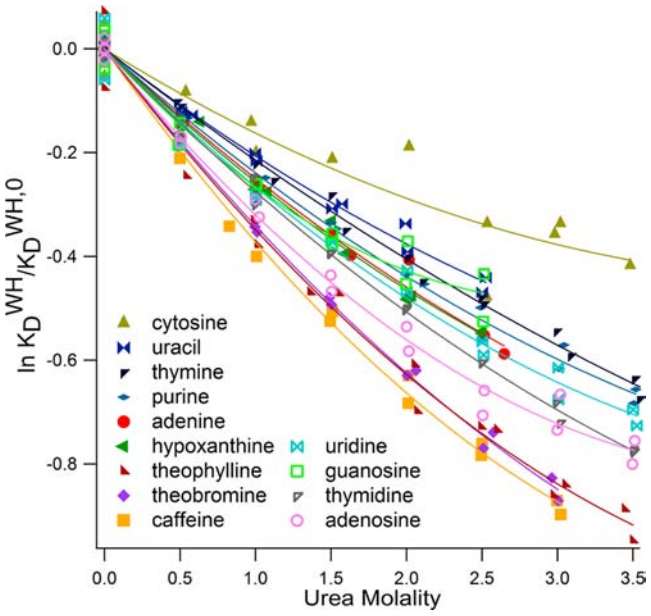

Figure 1. Logarithm of the macroscopic distribution coefficient ratio $K_D^{WH}/K_D^{WH,0}$ vs urea molality, where K_D^{WH} is the molal scale distribution coefficient $(m_2^{hex}/m_2^{aq})_{eq}$ for a nucleobase or base analogue between hexanol-rich and water-rich phases in the presence of urea and $K_D^{WH,0}$ is the distribution coefficient for the nucleobase between hexanol-rich and water-rich phases in the absence of urea. Initial slopes are used to determine μ_{23}/RT (eq 2).

4.1.2. Vapor Pressure Osmometry Studies. Interactions of urea with the modestly soluble disodium salts of the 5′-NMPs were quantified from VPO measurements by determining the osmolality difference ΔOsm (eq 4) as a function of m_2m_3, the product of the 5′-NMP and urea molalities (Figure 2). Linear regression of the data in Figure 3 with intercepts fixed at zero yields values of μ_{23}/RT (eq 4) summarized in Table 1. The negative slopes in Figure 2 indicate a net favorable preferential interaction of urea with the 5′-NMP anion and the two Na^+ ions.

dx.doi.org/10.1021/ja400965n | J. Am. Chem. Soc. 2013, 135, 5828−5838

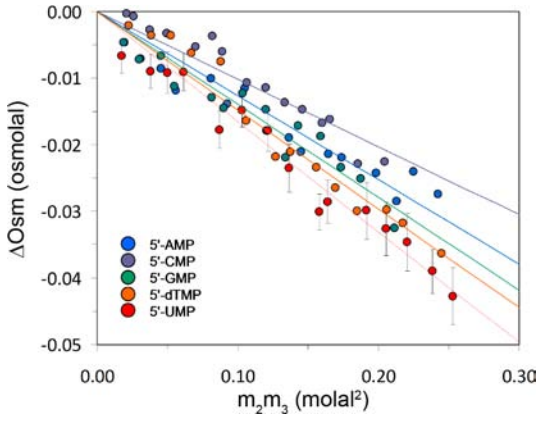

Figure 2. Excess osmolality ΔOsm (eq 5) of disodium salts of 5′-NMPs in aqueous urea solutions as a function of m_2m_3, the product of the molalities of 5′-NMP (m_2) and urea (m_3). Slopes are μ_{23}/RT (eq 4).

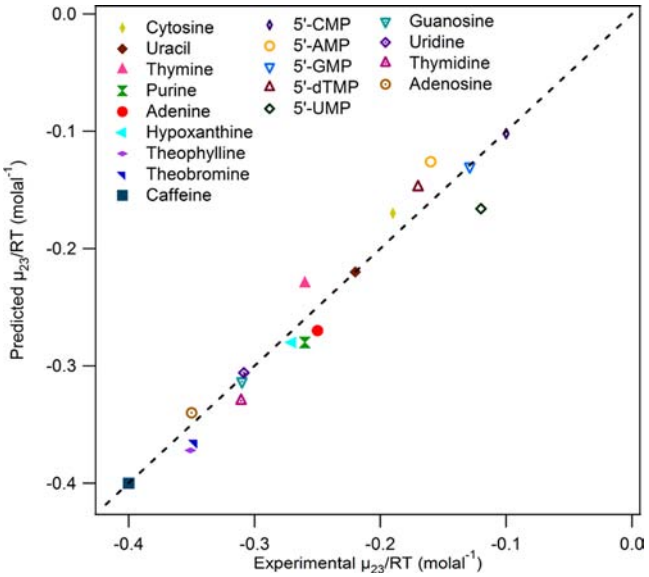

Figure 3. Predicted vs observed values of μ_{23}/RT for interactions of urea with model compounds (see Table 1). The line represents equality of predicted and observed values.

4.2. Interpreting Preferential Interactions (μ_{23}/RT Values) between Urea and Nucleic Acids. Values of μ_{23}/RT for interactions between urea and nucleobases/base analogues/nucleosides/nucleotides obtained from the slopes of plots of VPO and partitioning data (Figures 2 and 3) are summarized in Table 1. The groups in Table 1 (nucleobases, nucleosides, mononucleotides) are arranged in order of increasing molecular weight and ASA (Table S1, Supporting Information). Since interactions of urea with all but one type of organic surface investigated to date (the exception being cationic N)[4] are favorable, we expect urea to have a more favorable interaction (more negative μ_{23}/RT value) with larger compounds. Indeed, uridine, deoxythymidine, and adenosine μ_{23}/RT values are more favorable (more negative) than uracil, thymine, and adenine μ_{23}/RT values by approximately 0.1 m^{-1}, presumably due to a favorable interaction with the sugar ASA on nucleosides. However, urea exhibits less favorable interactions with the 5′-NMP disodium salts than with corresponding nucleobases and nucleosides. This is consistent with the strong unfavorable interaction of urea with Na^+ ions deduced from model compound data[4] ($2\beta_{Na^+}$ = 0.197 ± 0.028 m^{-1}). Correction for this effect shows that μ_{23}/RT values for interactions of urea with the 5′-UMP dianion (−0.363 ± 0.057 m^{-1}) and 5′-dTMP dianion (−0.345 ± 0.031 m^{-1}) are more negative than for the nucleosides uridine (−0.31 ± 0.02 m^{-1}) and deoxythymidine (−0.31 ± 0.02 m^{-1}). While the μ_{23}/RT value calculated for the 5′-AMP dianion (−0.323 ± 0.030 m^{-1}) is less negative than for the nucleoside adenosine (−0.35 ± 0.02 m^{-1}), both are more negative than μ_{23}/RT for the nucleobase adenine (−0.27 ± 0.01 m^{-1}).

Qualitative analysis of these μ_{23}/RT values leads to the following picture of the preferential interactions of urea with nucleic acid base, sugar, and phosphate functional groups:

(i) Values of μ_{23}/RT for nucleobases, base analogues, nucleosides, and Na_2NMPs are all negative, showing that preferential interactions of urea with all model compounds studied are favorable. Therefore, urea must interact favorably with most if not all types of nucleic acid surfaces.

(ii) Values of μ_{23}/RT for purine and pyrimidine bases and base analogues with similar functional groups (e.g., adenine vs cytosine, 5′-AMP vs 5′-CMP, or hypoxanthine vs uracil) reveal a more favorable μ_{23}/RT of the purines (with two fused heterocyclic aromatic rings) than the pyrimidines (with one heterocyclic aromatic ring), indicating a favorable interaction of urea with a ring surface.

(iii) Values of μ_{23}/RT for the nucleic acid bases adenine, thymine, and uracil are less negative (less favorable) than the corresponding values for the nucleosides adenosine, thymidine, guanosine, and uridine, indicating that urea has a favorable interaction with the nucleoside sugar.

(iv) In general, values (Table 3) of μ_{23}/RT become more negative (more favorable) as more functional groups are added to the heterocyclic ring. Comparing purines, μ_{23}/RT values for caffeine, theobromine, and theophylline, with 4−5 groups attached to the ring, are significantly more negative than μ_{23}/RT values for hypoxanthine, adenine, and purine (which have 0−1 group attached). This indicates a favorable preferential interaction of urea with these functional groups that is large enough to compensate for the loss of favorable urea−ring interaction resulting from the steric effect of these groups.

(v) Values of μ_{23}/RT for uracil (also 5′-UMP) are more negative than for cytosine (also 5′-CMP). Here the chemical difference is between a carbonyl oxygen (uracil) and an amino nitrogen (cytosine); both nucleobases display similar amounts of ring ASA. Therefore, urea must interact more favorably with carbonyl oxygen than amino nitrogen, analogous to the more favorable interaction of urea with amide O than with amide N on protein model compounds.[4]

(vi) The value of μ_{23}/RT for thymine is slightly more negative than for uracil. The addition of the methyl group to the C5 position of uracil to give thymine adds aliphatic ASA but eliminates aromatic ring ASA. The elimination of the favorable interaction of this aromatic ASA with urea is found to be compensated completely by a favorable interaction of urea with the added methyl ASA.

dx.doi.org/10.1021/ja400965n | J. Am. Chem. Soc. 2013, 135, 5828−5838

Because in general each functional group affects the accessible surface area of neighboring groups, a quantitative analysis of the interactions of urea with nucleobases cannot be based solely on functional groups, but must incorporate the accessibility of these groups, as in the next section.

4.3. Analysis of μ_{23}/RT: Interactions of Urea per Unit Area of Each Nucleic Acid Functional Group. Using ASA data and the experimentally determined μ_{23}/RT values, we globally fit the model compound data to eq 3 as described in the Experimental Section to determine interaction potentials α_i for the interaction of urea with each type of nucleic acid surface (Table 2). The fits for other surface types are unaffected by grouping ring C and N and sugar C and O together. Urea interacts favorably (negative α_i values) with all types of nucleic acid surfaces studied here, interacting most favorably with the aromatic ring and the methyl group attached to it.

Table 2. Values of the Interaction Potential α_i for the Interaction of Urea with Nucleic Acid and Protein Surface Types

nucleic acid surface type	$\alpha_i \times 10^4$ (m^{-1} Å^{-2})	protein surface type[a]	$\alpha_i \times 10^4$ (m^{-1} Å^{-2})
aromatic ring (C,N)	−10.9 ± 0.7	aromatic C	−8.9 ± 0.5
ring methyl	−12.0 ± 1.0	aliphatic C	−1.1 ± 0.5
carbonyl O	−6.2 ± 1.9	amide O	−8.5 ± 1.8
amino N	−2.8 ± 1.9	amide N	−3.7 ± 2.2
phosphate O	−5.8 ± 1.2	carboxylate O	−3.7 ± 1.6
sugar	−6.6 ± 0.7		

[a]From ref 4 with minor revision (see the Supporting Information).

The α_i values in Table 2 were used to predict μ_{23}/RT values for interactions of urea with all model compounds in the training set. Experimental and calculated values are given in Table 1 and compared in Figure 3; agreement is very good. The average deviation of calculated values from experimental values is ±8%, indicating that we have successfully developed the ability to predict interactions of urea with compounds displaying nucleic acid surface types. The next step is to use urea α_i values to predict the effects of urea on nucleic acid processes such as RNA and DNA duplex formation (see the section "Effect of Urea on DNA and RNA Dodecamer Melting Results").

To gain a molecular perspective of the interaction of urea with each functional group, these α_i values are interpreted using the solute partitioning model in terms of a microscopic partition coefficient defined as the ratio of the concentration of solute in the local hydration water and in bulk water ($K_p^{SPM} = m_3^{loc}/m_3^{bulk}$) as described in detail in refs 4, 5, 40, and 41. A positive $\alpha_i \times 10^4$ value of approximately 30 m^{-1} Å^{-2} was obtained for Na_2SO_4, corresponding to complete exclusion of both Na^+ and SO_4^{2-} ions from approximately two layers of water hydrating a hydrocarbon surface ($K_p = 0$), while the most negative value obtained to date for chemical interactions is −68 m^{-1} Å^{-2} for the accumulation of the three ions of Na_2SO_4 at an amide surface ($K_p = 3.49$);[7] compared to these large α_i values, interactions of urea are relatively subtle.

Lambert and Draper[18] obtained VPO data for urea–potassium dimethyl phosphate interactions and combined this with literature solubility and VPO data to determine contributions to μ_{23}/ASA (equivalent to $(RT)\alpha_i$ values) for the interaction of urea with a unit area of nucleic acid base, sugar, and phosphate surface. These can be compared with our α_i values determined from a different data set.

(i) Their α_i value for anionic phosphate O (-6.1×10^{-4} m^{-1} Å^{-2}, obtained from potassium dimethyl phosphate VPO data by correcting for the interaction of urea with K^+ ion, ester O, and methyl groups using α_i values from ref 4),[18] is the same within uncertainty as that determined here (Table 2). Since very different compounds and analyses are used, this agreement is very encouraging.

(ii) Analysis of uncorrected solubility data for adenine and cytosine in aqueous urea solutions[42] yields α_i values for adenine of -8.9×10^{-4} m^{-1} Å^{-2} and for cytosine of -7.6×10^{-4} m^{-1} Å^{-2}. Lambert and Draper[18] corrected these solubility data for nucleobase self-interaction due to stacking (estimated from purine and cytidine VPO data because adenine and cytosine are too insoluble for VPO) to obtain nucleobase α_i values of -11×10^{-4} and -10×10^{-4} m^{-1} Å^{-2}, respectively. Our nucleobase α_i values for adenine (-9.5×10^{-4} m^{-1} Å^{-2}) and cytosine (-6.5×10^{-4} m^{-1} Å^{-2}) determined from the μ_{23}/RT values in Table 1 (obtained using the hexanol–water distribution assay at low nucleobase concentrations where stacking is negligible) are closer to the values determined from the uncorrected solubility data, indicating that the correction for stacking may be too large. Lambert and Draper[18] determined an average α_i value for nucleic acid bases (-11×10^{-4} m^{-1} Å^{-2}) from these adenine and cytosine data. Because we quantified interactions of urea with nine nucleobases and base analogues, we obtain values for the individual ring functional groups and the ring ASA.

(iii) The sugar α_i value (-2.0×10^{-4}) predicted[18] from sugar ASA and model compound VPO data for glycerol and sucrose (ref 4) is only 1/3 as large in magnitude as the sugar α_i value in Table 2, which is determined from nucleosides and mononucleotides. This is surprising since it indicates a failure of the assumption of additivity, which generally is found to be valid[1,4–7] as Figure 3 indicates. This context dependence indicates that the neighboring nucleic acid base affects how the sugar interacts with urea, as is observed with the ring methyl (see below). This does not affect the use of eq 3 to analyze the data here as the context of the sugar is always the same.

4.4. Comparison of α_i Values and Their Molecular Interpretation for Interactions of Urea with Protein and Nucleic Acid Functional Groups. Proteins and nucleic acids contain similar types of functional groups. How do interaction potentials α_i for the interaction of urea with each of these similar groups compare (Table 2)? Can these nucleic acid α_i values be interpreted in terms of noncovalent interactions of urea with the nucleic acid functional groups, as has been reported for interactions of urea and GB with protein functional groups?[4]

4.4.1. Aromatic Ring C and N. Table 2 shows that urea has a more favorable preferential interaction with the heterocyclic rings found on nucleic acid bases ($K_p = 1.34$), which can accept hydrogen bonds to the π-system as well as hydrogen bonds to or from the ring N atoms, than with homocyclic aromatic rings of tyrosine and phenylalanine residues on proteins ($K_p = 1.28$), suggesting that urea may have a preference for ring N over ring C. The interaction of urea with both ring types may involve a hydrogen bond donated from the urea amide N to the π-system

dx.doi.org/10.1021/ja400965n | J. Am. Chem. Soc. 2013, 135, 5828–5838

Table 3. Experimentally Determined Urea *m*-Values/*RT* for DNA and RNA Duplex Formation[a]

sequence	GC content (%)	temp[a] (°C)	van't Hoff ΔH_{obsd}[b] (kcal mol^{-1})	*m*-value[c] (kcal mol^{-1} *m*$^{-1}$)	predicted *m*-value for 75% stacked single strands[d] (kcal mol^{-1} *m*$^{-1}$)
DNA Duplexes					
5′-d(GAAATTATAAAC)-3′	17	15		0.75 ± 0.07	0.81 ± 0.09
5′-d(GAAAGTATAAAC)-3′	25	18		0.85 ± 0.02	0.81 ± 0.09
5′-d(GAAAGTAGAAAC)-3′	33	18		0.72 ± 0.04	0.79 ± 0.09
5′-d(GCAAAGTAAACG)-3′	42	30		0.81 ± 0.04	0.80 ± 0.10
5′-d(GCAAAGCAAACG)-3′	50	41	−18.7 ± 0.7	0.73 ± 0.06	0.79 ± 0.10
5′-d(GCATAGCATACG)-3′	50	41	−17.5 ± 1.0	0.58 ± 0.05	0.80 ± 0.10
RNA Duplexes					
5′-r(GAAAGUAGAAAC)-3′	33	41	−23.1 ± 0.1	0.98 ± 0.03	0.78 ± 0.09
5′-r(GCAAAGCAAACG)-3′	50	52	−25.0 ± 0.1	0.93 ± 0.03	0.79 ± 0.09
5′-r(GCAUAGCAUACG)-3′	50	52	−24.1 ± 0.2	0.87 ± 0.04	0.79 ± 0.09
5′-r(GCGAAGCCAACG)-3′	67	63	−26.4 ± 0.5	0.84 ± 0.03	0.77 ± 0.10
5′-r(GCGCCGCCGGCG)-3′	100	81	−27.4 ± 0.5	0.59 ± 0.04	0.77 ± 0.11

[a]*m*-values for duplex formation from thermal denaturation experiments determined at the temperature with an 0.80 fraction of the duplex intact in 0 *m* urea. *m*-values from isothermal titration experiments determined at the temperature with a 1.0 fraction of the duplex intact in 0 *m* urea. [b]van't Hoff enthalpies of duplex formation calculated as described in the Experimental Section from thermal melts in the absence of urea. [c]First four *m*-values determined from isothermal urea titrations. All other *m*-values determined from thermal melts. For all experiments, the concentration of DNA and RNA strands used is ∼2.5 μM. [d]Determined from the average of the *m*-value predicted for half-stacked single strands and the *m*-value predicted for fully stacked single strands (Table S4, Supporting Information). Prediction uses urea α_i values determined at 25 °C (Table 2) and so is most applicable to the first four entries.

of the aromatic ring,[43] a partial cation−π interaction with the urea amide N,[44] or a π−π stacking interaction of urea with the ring (observed in simulations of urea with an RNA hairpin[45] and with 5′-NMPs, detailed in the Supporting Information), all allowing urea to interact more favorably with the ring than water does.

4.4.2. Carbonyl O. The urea−carbonyl O preferential interaction (K_p = 1.19) is slightly less favorable than that of urea with amide O (K_p = 1.28). As with amide O, the urea−carbonyl O interaction can be interpreted as a hydrogen bond donated from the urea NH_2. Moreover, we would expect the carbonyl O groups attached to the heterocyclic aromatic ring N atoms to behave similarly to amide O because they can participate in resonance structures with the ring in the same way that amide O can participate in resonance structures with amide N.

4.4.3. Amino N. Urea can act as a hydrogen bond donor and acceptor with amino N (K_p = 1.09), like with amide N (K_p = 1.10). Amino N groups can also participate in resonance structures with the ring as amide N groups do with amide O, and we find similar weak favorable interactions of urea with these two groups. Urea interacts less favorably with amino N than carbonyl O. We interpreted the less favorable interaction of urea with amide N than amide O as a favorable urea O−amide N hydrogen bond counteracted by an unfavorable urea N−amide N hydrogen bond. Likewise, we expect a favorable interaction between urea amide O and amino N similar in magnitude to the urea−carbonyl O interaction, indicating that while urea O−amino N hydrogen bonds are favorable relative to those with water, urea NH_2−amino N hydrogen bonds are disfavored in comparison to hydrogen bonds with water.

4.4.4. Aliphatic C. Urea has a moderately favorable preferential interaction with the methyl group attached to nucleic acid heterocyclic rings (K_p = 1.37, similar to the interaction with the ring itself). Surprisingly, the α_i value for the interaction of urea with an aliphatic C surface on the nucleobase aromatic ring (proportional to $K_p - 1$) is almost an order of magnitude larger than for ordinary aliphatic C (K_p = 1.03). Urea also has a larger than expected interaction with the methyl group on toluene and the tetramethylbutyl group on the phenyl ring of Triton X-100 micelles (see the Supporting Information for details), indicating that urea has a more favorable interaction with an aliphatic hydrocarbon that is a substituent on an aromatic ring, which could affect the electron distribution of the attached methyl groups through both inductive and resonance effects. Additionally, urea could be involved in a π−π interaction with the ring[45] while interacting with the methyl group attached to the ring, making the interaction more favorable than that with water, which lacks a π-system. Since the only aliphatic groups considered explicitly here are these ring methyls, this deviation from additivity does not affect the application of eq 3 to the nucleobase/base analogue data set.

Examples of nonadditivity have been found for certain Hofmeister salt ions as well. Consistent with the stacking hypothesis, Hofmeister ions with a π-system that can stack on the ring (e.g., GuH^+) also have a more favorable interaction with the ring methyl than with aliphatic C while ions lacking a π-system do not (see the Supporting Information). We do not see the same effect of the ring on the preferential interaction of urea or GuH^+ salts with ring moieties with which they can hydrogen bond (amino N, carbonyl O), suggesting that stacking only significantly affects ring moiety interactions relative to those with water when stronger hydrogen-bonding interactions (which water can also participate in) are not possible. In another example of context dependence involving a π-system, spectroscopic studies and MD simulations[46] indicate that interactions of Hofmeister anion SCN^- (also I^-) with the methylene C adjacent to the amide π-system of the peptide backbone are more favorable than their interactions with side chain aliphatic C.

4.4.5. Phosphate O. Phosphate O and carboxylate O are both anionic O functional groups, but the interaction of urea with phosphate O is somewhat more favorable (K_p = 1.18). We have interpreted the favorable interaction of urea with carboxylate O (K_p = 1.13) in terms of a hydrogen bond donated from urea $-NH_2$, so perhaps the hydrogen bond with

dx.doi.org/10.1021/ja400965n | J. Am. Chem. Soc. 2013, 135, 5828−5838

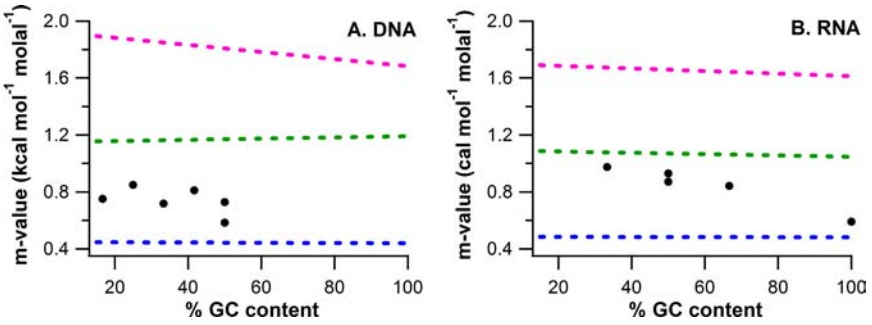

Figure 4. Predicted (dashed lines) and observed (black points) urea *m*-values for formation of 12 bp duplex DNAs (A) or RNAs (B) from stacked (blue), half-stacked (green), or unstacked (pink) single strands vs GC content (%) of DNA oligomers.

phosphate O is stronger due to its larger partial negative charge (2/3 vs 1/2).

4.4.6. Sugar. The sugar ring consists of highly correlated C and O groups with an O:C ASA ratio of 1.2−1.5 for all 5′-NMPs and nucleosides except 5′-dTMP and deoxythymidine, which had an O:C ratio of 0.6 (but were still well fit by the same sugar α_i value). The interaction of urea with sugar (K_p = 1.21) is similarly favorable to the interaction of urea with the other O surface types in the data set (carbonyl O, phosphate O) despite the additional hydrocarbon ASA on the sugar ring. The sugar K_p value predicted from sucrose and glycerol model compound data as described above is less favorable. This could be another situation where the context of a group affects its interactions with urea. Whether the significant context is the constrained geometry of the sugar ring or its proximity to the π-system of the base ring remains to be determined.

Molecular dynamics simulations using the Amber force field for urea were performed to visualize the accumulation of urea at the 5′-NMPs studied here and are described in the Supporting Information. They indicate that urea can participate in the hydrogen-bonding and stacking interactions that we discuss above. The interaction potentials in Table 2 can be used to tune MD force fields to allow for more quantitative thermodynamic predictions to be made from the simulations.

4.5. Effect of Urea on DNA and RNA Dodecamer Melting. To test the ability of urea α_i values (Table 2) to predict or interpret the effects of urea on nucleic acid processes, we quantified *m*-values for the effect of urea on DNA and RNA dodecamer duplex formation by urea titration and thermal denaturation. Urea destabilizes all RNA and DNA duplexes, indicating favorable interactions between urea and ΔASA, the surface area of the nucleic acid (mostly of the nucleobases) that becomes water accessible during the melting process. Values of $\Delta G^\circ_{obsd} = -RT \ln K_{obsd}$ for each oligomer, interpolated from melting curves to a selected reference temperature in the transition region of the oligomer at all urea concentrations studied (as described in the Experimental Section), were plotted as a function of urea molality to obtain the urea *m*-value for duplex formation from the slope (Figure S2, Supporting Information). All *m*-values (Table 3) are positive due to favorable interactions between urea and the surface described by the ΔASA. Values of ΔH_{obsd} for formation of oligomers studied by thermal denaturation, determined from van't Hoff plots as described in the Experimental Section, are also listed in Table 3. Like $d\Delta G^\circ/dm_3$ (the *m*-value), $d\Delta H^\circ/dm_3$ derivatives are positive but are not accurately enough determined to be able to dissect enthalpic and entropic contributions to the urea *m*-value as was done for protein unfolding.[47] RNA K_{obsd} values were determined at higher temperatures because RNA duplex dodecamers had higher T_m values than DNA duplex dodecamers with a similar nucleobase sequence, as expected.[48]

Urea−nucleic acid α_i values (Table 2) predict urea *m*-values for forming these duplexes using the ΔASA for duplex association from single strands (eq 3). Previously, Guinn et al. predicted protein folding *m*-values using urea−protein functional group interaction potentials, obtaining good agreement using an extended (unstructured) model for the unfolded state.[4] Here, because the amount of single-stranded stacking is expected to be large, we calculated ΔASA values for DNA and RNA melting determined assuming single strands in fully stacked and half-stacked states to compare with predictions for unstacked states (see the Experimental Section and the Supporting Information, Table S3). We divided ΔASA into the same functional groups as the nucleobases/base analogues and 5′-NMPs. Our ΔASA values calculated for a model with the half-stacked DNA and RNA single strands are in good agreement with those of Hong et al.[25] Most of the ΔASA arises from exposure of heterocyclic ring, carbonyl O, and amino N groups; a small reduction in phosphate oxygen surface area is also predicted.

Using these ΔASA values and the urea−nucleic acid α_i values in Table 2, we predicted *m*-values for the effect of urea on RNA and DNA duplex formation assuming different extents of residual stacking in the single strands at the temperature where K_{obsd} is determined (Table S4, Supporting Information). We compare urea *m*-values determined at different temperatures here because we expect (and observe) that urea *m*-values for nucleic acid duplex formation are less temperature dependent than urea *m*-values/*RT* (see the Supporting Information). Our α_i values are determined at 25 °C, while the experimental *m*-values were determined at temperatures ranging from 15 to 81 °C due to the large range of T_m values for the dodecamers studied (Table 3). These predictions are most applicable to the first four entries in Table 2, which are determined at ∼25 °C.

m-values predicted for DNA and RNA duplex formation assuming completely stacked single strands do not show a significant dependence on nucleobase composition (Figure 4, blue dashed lines). *m*-values predicted assuming completely unstacked nucleobases (Figure 4, pink dashed lines) show no nucleobase composition dependence for RNA and a small reduction in the magnitude of the *m*-value with increasing GC content (%) for DNA due to the smaller contribution to the ΔASA from thymine, the ring methyl of which interacts very favorably with urea. Experimental *m*-values scatter between the predictions obtained for completely stacked and half-stacked single strands and show little nucleobase composition depend-

dx.doi.org/10.1021/ja400965n | J. Am. Chem. Soc. 2013, 135, 5828−5838

Table 4. Experimentally Determined Urea *m*-Values for RNA Duplex Formation[17] and the Amount of Stacking Predicted

sequence	exptl *m*-value (kcal mol^{-1} m^{-1})	temp (°C)	stacking[a] (%)
5′-r(GCAGUAGUCGACUACUGC)-3′	1.17	70	80
5′-r(GCAGUAGCUACUGC)-3′	1.06	60	70
5′-r(GCAGUACUGC)-3′	0.84	50	60
5′-r(GUAAUAUUAC)-3′	0.74	20	69
5′-r(GCAUGC)-3′	0.64	20	30

[a]Predicted amount of residual stacking (%) in single strands in transition.

ence. *m*-values for all DNAs are best predicted assuming 70−90% stacking. *m*-values for most RNAs are best predicted assuming 60−70% stacking, while the *m*-value for the 100% GC RNA oligomer is best predicted assuming almost 100% stacking. The four DNA oligomers studied at 15−30 °C (closest to 25 °C, the temperature at which the urea interaction potentials used to predict *m*-values were obtained) have quite similar urea *m*-values (Table 3), indicating no large effect of nucleobase composition.

Stacking can be estimated directly from hyperchromicity by assuming the absorbance of duplex DNA represents the absorbance of a completely stacked DNA while the absorbance of NMPs from a DNA digest represents the absorbance of completely unstacked single strands. Using this technique, Holbrook et al. found a 66% GC DNA single strand is 75% stacked at 40 °C, consistent with what we see in Figure 4 for the more GC-rich DNAs studied at 41 °C, and stacking decreases from 89% at 10 °C to 52% at 80 °C (the temperature range studied here); all our DNAs and RNAs fall within this range of stacking.[49] Lambert and Draper[18] predicted *m*-values for the effect of urea on melting a series of RNAs, some containing extensive tertiary structure, using their more course-grained model of nucleic acid components. They found that *m*-values were better predicted when they used an A-form single-stranded helix as a model for unfolded RNA than an extended unstacked model, consistent with our prediction of significant single-strand stacking.

Different-single stranded nucleic acid homopolymers exhibit different degrees of stacking. Poly(T), poly(U), and poly(C) exhibit essentially no stacking at 25 °C, while poly(A) stacks extensively.[50−52] Hence, the amount of stacking in our single-stranded oligomers may depend in part on the nucleobase sequence, perhaps explaining the scatter in Figure 4. The *m*-values for RNAs were determined at higher temperature due to their increased thermal stability, which could explain why their *m*-values are more accurately predicted by invoking a smaller extent of stacking. Because urea promotes exposure of the nucleic acid surface, urea is expected to reduce residual stacking in the unfolded form. This has not been observed, and the observation that urea *m*-values are independent of urea concentration up to at least 7 M urea for RNA duplexes and yeast tRNA^{Phe} indicates that the ΔASA of unfolding is not a significant function of the urea concentration.[17] Likewise, the linearity of protein folding *m*-values[2] indicates no significant urea concentration dependence of the protein denatured state ensemble even though we might expect the denatured state to become more solvent accessible at higher urea concentrations.

Shelton et al. measured urea *m*-values for melting a series of five RNA duplexes from 6 to 18 base pairs in length; four of their duplexes are approximately 60% GC, and one is 20% GC.[17] They found that the *m*-value increased in proportion to the length (i.e., to ΔASA).[2] From estimates of ΔASA of melting of the duplexes studied by Shelton et al., assuming stacked, half-stacked. and unstacked nucleobases in the single strands, we predict *m*-values using the urea α values of Table 2. Comparison of predicted and experimental *m*-values yields predictions for the amounts of residual stacking in the single strands (Table 4). For all but the shortest duplex, the predicted amount of single-strand stacking is consistent with that determined for the dodecamers investigated here (Figure 4).

5. CONCLUDING DISCUSSION

We demonstrate that urea interacts favorably with all nucleic acid surface types, relative to interactions with water, and that urea destabilizes nucleic acid duplexes by its favorable interactions with both the ring and functional groups of nucleobases which become solvent accessible in the single-stranded state. Per unit of accessible surface area, the most favorable interactions of urea are with the heterocyclic aromatic rings of all bases and with the methyl group of thymine. We use these data to probe the extent of unstacking in formation of DNA and RNA duplexes and find that a large amount of residual stacking (60−90%, depending on the nucleobase composition and sequence) in the individual single strands is necessary to obtain agreement between observed and predicted urea *m*-values. Once dissected into individual interactions of amide O and N (by studying interactions of a compound with a different O:N ratio, such as malonamide, with the same set of model compounds),[1] these data will provide significant information about interactions between the protein backbone and nucleic acids in protein−nucleic acid complexes.

Now that interactions of urea with both nucleic acid and protein[4] functional groups have been quantified, urea will be useful as one of a set of solute probes being developed to detect and characterize large-scale conformational changes and formation of new interfaces in the steps of protein and nucleic acid mechanisms. For urea and the osmolyte stabilizer GB, thermodynamic *m*-values for folding of globular proteins and for formation of a repression complex between the lac repressor protein and lac operator DNA are well-predicted from α values for these solutes and structural information.[1,4,6] Kinetic and/or thermodynamic *m*-values have been determined for urea, GB, and potassium glutamate (compared with KCl to eliminate polyelectrolyte effects of K^+ and thereby compare the physiological anion glutamate(−) with the laboratory anion Cl^-) for various steps in forming a transcription initiation complex between RNA polymerase and promoter DNA.[53,54] The lack of large effects of any of these solutes on the kinetics and thermodynamics of the step in which the 13 base pairs of DNA are opened provides one line of evidence that opening occurs in the cleft of RNA polymerase and not in a solution environment. The very large stabilizing effects of GB and glutamate (relative to Cl^-), and the large destabilizing effect of urea, on the step that converts the initial unstable open complex to a highly stable open complex, increasing its lifetime from 1 s to >10^5 s at the promoter investigated, provide the

dx.doi.org/10.1021/ja400965n | J. Am. Chem. Soc. 2013, 135, 5828−5838

best evidence available to date that this step involves folding and assembly of 100−150 residues of RNA polymerase to form a jaw/clamp structure on the downstream duplex DNA after opening.[22,54−56] Even before full information about solute interactions with protein and nucleic acid surfaces is available, kinetic *m*-value studies can provide qualitative answers about steps with large conformational changes or new interfaces in other assembly processes and the operation of other protein machines, such as the spliceosome.[57] The data obtained here will help to provide quantitative information about the types and amounts of surfaces buried or exposed in these processes.

■ ASSOCIATED CONTENT

Supporting Information

Details of the materials used, 5′-NMP VPO sample preparation, assumptions in determining μ_{23}/RT from K_D^{WH} values, determining molal scale K_D^{WH} values, distribution assay data analysis, determining urea in the hexanol phase, controls for the distribution assay, DNA and RNA dodecamer sample preparation, reanalysis of the Guinn et al.[4] data, urea−aliphatic C interactions, determining interactions of urea with Triton micelles, molecular dynamics simulations of 5′-NMPs, determining the effect of urea on the salt dependence of melting, and the temperature dependence of *m*-values vs *m*-values/*RT*, tables containing contributions to the ASA of model compounds, pseudorotation phase angle and glycosyl torsion angle distribution in 5′-mononucleotide molecular dynamics simulations, contributions to ΔASA for formation of DNA and RNA duplexes assuming 100%, 50%, and 0% stacked nucleobases in the single strands, experimental and predicted *m*-values for the effect of urea on helix formation assuming different amounts of stacking, and values of μ_{23}/RT for the interaction of GuHCl with nucleic acid bases and base analogues determined from hexanol/water two-phase partitioning and solubility assays, and figures showing plots from the two-phase distribution assay with urea and caffeine, plots of ΔG_{obsd} vs urea molality for duplex formation by DNA and RNA, a plot of ΔOsm determined by VPO against m_2m_3 for urea with thymidine and uridine, plots of the log of the macroscopic distribution coefficient ratio $K_D^{WH}/K_D^{WH,0}$ vs GuHCl molality, plots of the negative log of cmc vs urea molality for Triton X-100 and Triton X-305, and average urea oxygen and nitrogen density around adenine and uracil from 5′-NMP MD simulations. This material is available free of charge via the Internet at http://pubs.acs.org.

■ AUTHOR INFORMATION

Corresponding Author

mtrecord@wisc.edu

Author Contributions

‖E.J.G., J.J.S., and H.K.C. contributed equally to this work.

Notes

The authors declare no competing financial interest.

■ ACKNOWLEDGMENTS

We thank D. B. Knowles and M. W. Capp for helpful discussions in developing the distribution assay and the reviewers for valuable comments on the manuscript. This research was supported by National Institutes of Health Grants GM 47022 (to M.T.R.) and R15-GM093331 (to J.J.S. and G.W.M.). This work was also supported in part by a grant to St. Olaf College from the Howard Hughes Medical Institute through the Undergraduate Science Education Program. Computer simulations were performed at the University of Minnesota Supercomputing Institute.

■ REFERENCES

(1) Record, M. T. J.; Guinn, E.; Pegram, L.; Capp, M. *Faraday Discuss.* **2013**, *160*, 9.
(2) Myers, J. K.; Pace, C. N.; Scholtz, J. M. *Protein Sci.* **1995**, *4*, 2138.
(3) Courtenay, E. S.; Capp, M. W.; Record, M. T. *Protein Sci.* **2001**, *10*, 2485.
(4) Guinn, E. J.; Pegram, L. M.; Capp, M. W.; Pollock, M. N.; Record, M. T. *Proc. Natl. Acad. Sci. U.S.A.* **2011**, *108*, 16932.
(5) Pegram, L. M.; Record, M. T. *J. Phys. Chem. B* **2008**, *112*, 9428.
(6) Capp, M. W.; Pegram, L. M.; Saecker, R. M.; Kratz, M.; Riccardi, D.; Wendorf, T.; Cannon, J. G.; Record, M. T., Jr. *Biochemistry* **2009**, *48*, 10372.
(7) Pegram, L. M.; Wendorff, T.; Erdmann, R.; Shkel, I.; Bellisimo, D.; Felitsky, D. J.; Record, M. T. *Proc. Natl. Acad. Sci. U.S.A.* **2010**, *107*, 7716.
(8) Hong, J.; Capp, M. W.; Anderson, C. F.; Saecker, R. M.; Felitsky, D. J.; Anderson, M. W.; Record, M. T. *Biochemistry* **2004**, *43*, 14744.
(9) Felitsky, D. J.; Cannon, J. G.; Capp, M. W.; Hong, J.; Wynsberghe, A. W. V.; Anderson, C. F.; Record, M. T. *Biochemistry* **2004**, *43*, 14732.
(10) Sagle, L. B.; Zhang, Y.; Litosh, V. A.; Chen, X.; Cho, Y.; Cremer, P. S. *J. Am. Chem. Soc.* **2009**, *131*, 9304.
(11) Lim, W. K.; Rosgen, J.; Englander, S. W. *Proc. Natl. Acad. Sci. U.S.A.* **2009**, *106*, 2595.
(12) Babayan, Y. S. *Mol. Biol.* **1988**, *22*, 1204.
(13) Aslanyan, V. M.; Babayan, Y. S.; Arutyunyan, S. G. *Biophysics* **1984**, *29*, 410.
(14) Klump, H.; Burkart, W. *Biochim. Biophys. Acta* **1977**, *475*, 601.
(15) Nordstrom, L. J.; Clark, C. A.; Andersen, B.; Champlin, S. M.; Schwinefus, J. J. *Biochemistry* **2006**, *45*, 9604.
(16) Schwinefus, J. J.; Kuprian, M. J.; Lamppa, J. W.; Merker, W. E.; Dorn, K. N.; Muth, G. W. *Biochemistry* **2007**, *46*, 9068.
(17) Shelton, V. M.; Sosnick, T. R.; Pan, T. *Biochemistry* **1999**, *38*, 16831.
(18) Lambert, D.; Draper, D. E. *Biochemistry* **2012**, *51*, 9014.
(19) Gluick, T. C.; Wills, N. M.; Gesteland, R. F.; Draper, D. E. *Biochemistry* **1997**, *36*, 16173.
(20) Gluick, T. C.; Yadav, S. *J. Am. Chem. Soc.* **2003**, *125*, 4418.
(21) Hong, J.; Capp, M. W.; Saecker, R. M.; Record, M. T. *Biochemistry* **2005**, *44*, 16896.
(22) Kontur, W. S.; Saecker, R. M.; Davis, C. A.; Capp, M. W.; Record, M. T. *Biochemistry* **2006**, *45*, 2161.
(23) Knowles, D. B.; LaCroix, A. S.; Deines, N. F.; Shkel, I.; Record, M. T. *Proc. Natl. Acad. Sci. U.S.A.* **2011**, *108*, 12699.
(24) Hong, J.; Capp, M. W.; Anderson, C. F.; Record, M. T. *Biophys. Chem.* **2003**, *105*, 517.
(25) Hong, J.; Capp, M. W.; Anderson, C. F.; Saecker, R. M.; Felitsky, D. J.; Anderson, M. W.; Record, M. T. J. *Biochemistry* **2004**, *43*, 14744.
(26) Bevington, P. R.; Robinson, D. K. *Data Reduction and Error Analysis for the Physical Sciences*; McGraw-Hill, Inc.: New York, 1992.
(27) Tsodikov, O. V.; Record, M. T.; Sergeev, Y. V. *J. Comput. Chem.* **2002**, *23*, 600.
(28) Richards, F. M. *Annu. Rev. Biophys. Bioeng.* **1977**, *6*, 151.
(29) Case, D. A.; Darden, T. A.; T.E. Cheatham, I.; Simmerling, C. L.; Wang, J.; Duke, R. E.; Luo, R.; Crowley, M.; R. C..Walker; Zhang, W.; Merz, K. M.; B..Wang; Hayik, S.; Roitberg, A.; Seabra, G.; Kolossváry, I.; K. F..Wong; Paesani, F.; Vanicek, J.; X..Wu; Brozell, S. R.; Steinbrecher, T.; Gohlke, H.; Yang, L.; Tan, C.; Mongan, J.; Hornak, V.; Cui, G.; Mathews, D. H.; Seetin, M. G.; Sagui, C.; Babin, V.; Kollman, P. A. *AMBER 10*; University of California: San Francisco, 2008.

(30) Hubbard, S. J.; Thornton, J. M. *naccess*; Department of Biochemistry and Molecular Biology, University College London: London, 1993.
(31) DeLano, W. L. *The PyMOL User's Manual*; DeLano Scientific: San Carlos, CA, 2002.
(32) Shaw, W. H. R.; Bordeaux, J. J. *J. Am. Chem. Soc.* **1955**, *77*, 4729.
(33) Long, F. A.; McDevit, W. F. *Chem. Rev.* **1952**, *51*, 119.
(34) Nandi, P. K.; Robinson, D. R. *J. Am. Chem. Soc.* **1972**, *94*, 1308.
(35) Sykes, P. H.; Robertson, P. W. *J. Am. Chem. Soc.* **1933**, *55*, 2621.
(36) Smith, R.; Tanford, C. *Proc. Natl. Acad. Sci. U.S.A.* **1973**, *70*, 289.
(37) Shih, P.; Pederson, L. G.; Gibbs, P. R.; Wolfenden, R. *J. Mol. Biol.* **1998**, *280*, 421.
(38) Meylan, W. M.; Howard, P. H.; Boethling, R. S. *Environ. Toxicol. Chem.* **1995**, *15*, 100.
(39) Hansch, C.; Quinlan, J. E.; Lawrence, G. L. *J. Org. Chem.* **1968**, *33*, 347.
(40) Capp, M. W.; Pegram, L. M.; Saecker, R. M.; Kratz, M.; Riccardi, D.; Wendorff, T.; Cannon, J. G.; Record, M. T., Jr. *Biochemistry* **2009**, *48*, 10372.
(41) Courtenay, E. S.; Capp, M. W.; Saecker, R. M.; Record, M. T. *Proteins: Struct., Funct., Genet.* **2000**, *41*, 72.
(42) herskovits, T. T.; Bowen, J. J. *Biochemistry* **1974**, *13*, 5474.
(43) Levitt, M.; Perutz, M. F. *J. Mol. Biol.* **1988**, *201*, 751.
(44) Scrutton, N. S.; Raine, A. R. *Biochem. J.* **1996**, *319* (Part1), 1.
(45) Priyakumar, U. D.; Hyeon, C.; Thirumalai, D.; MacKerell, A. D. *J. Am. Chem. Soc.* **2009**, *131*, 17759.
(46) Rembert, K. B.; Paterova, J.; Heyda, J.; Hilty, C.; Jungwirth, P.; Cremer, P. S. *J. Am. Chem. Soc.* **2012**, *134*, 10039.
(47) Felitsky, D. J.; Record, M. T. *Biochemistry* **2003**, *42*, 2202.
(48) Kankia, B. I.; Marky, L. A. *J. Phys. Chem. B* **1999**, *103*, 8759.
(49) Holbrook, J. A.; Capp, M. W.; Saecker, R. M.; Record, M. T. *Biochemistry* **1999**, *38*, 8409.
(50) Bloomfield, V. A.; Crothers, D. M.; Tinoco, I. *Nucleic Acids: Structure, Properties and Functions*; University Science Books: Sausolito, CA, 2000.
(51) Goddard, N. L.; Bonnet, G.; Krichevsky, O.; Libchaber, A. *Phys. Rev. Lett.* **2000**, *85*, 2400.
(52) Riley, M.; Maling, B.; Chamberlin, M. J. *J. Mol. Biol.* **1966**, *20*, 359.
(53) Kontur, W. S.; Saecker, R. M.; Capp, M. W.; Record, M. T. *J. Mol. Biol.* **2008**, *376*, 1034.
(54) Kontur, W. S.; Capp, M. W.; Gries, T. J.; Saecker, R. M.; Record, M. T. *Biochemistry* **2010**, *49*, 4361.
(55) Drennan, A.; Kraemer, M.; Capp, M.; Gries, T.; Ruff, E.; Sheppard, C.; Wigneshweraraj, S.; Artsimovitch, I.; Record, M. T. *Biochemistry* **2012**, *51*, 9447.
(56) Saecker, R. M.; Record, M. T.; Dehaseth, P. L. *J. Mol. Biol.* **2011**, *412*, 754.
(57) Butcher, S. E.; Brow, D. A. *Biochem. Soc. Trans.* **2005**, *33*, 447.